

**Supplemental Information**

**Homomeric carboxy-terminal domain interactions mediate the formation of branched polymers of HIV-1 integrase induced by allosteric inhibitors.**

Kushol Gupta, Audrey Allen, Carolina Giraldo, Grant Eilers, Robert Sharp, Young Hwang, Hemma Murali, Katrina Cruz, Paul Janmey, Frederic Bushman, Gregory D. Van Duyne

**Table S1. Parameters derived from SANS fitting. Related to Figure 4.**

Sample	Concentration ( $\mu\text{M}$ )	Power Law <sup>1</sup>		Fractal Model <sup>2</sup>		
		Exponent	$\chi^2$	Fractal Dimension	Correlation Length ( $\text{\AA}$ )	$\chi^2$
IN <sup>F185H</sup> • BI-224436	100	4.5 $\pm$ 0.09	1.01	3.13 $\pm$ 0.03	705 $\pm$ 65.3	1.97
IN <sup>F185H</sup> • BI-D	100	3.9 $\pm$ 0.10	1.40	3.00 $\pm$ 0.01	1450.7 $\pm$ 74.4	1.60
IN <sup>Y15A,F185H</sup> • BI-224436	80	4.4 $\pm$ 0.04	1.21	3.05 $\pm$ 0.01	1466.6 $\pm$ 117.3	1.81
IN <sup>Y15A,F185H</sup> • BI-224436	221	4.1 $\pm$ 0.05	1.07	3.13 $\pm$ 0.01	1104.4 $\pm$ 154.7	1.31
IN <sup>Y15A,F185H</sup> • CX04328	80	4.2 $\pm$ 0.02	1.78	3.07 $\pm$ 0.01	1024.1 $\pm$ 79.4	2.50
IN <sup>Y15A,F185H</sup> • BI-D	80	4.3 $\pm$ 0.05	1.10	3.03 $\pm$ 0.01	2364.4 $\pm$ 172.6	1.02

1. Data fit in the Porod region, where  $0.003 \text{ \AA}^{-1} < q < 0.01 \text{ \AA}^{-1}$

2. Data fit where  $0.003 \text{ \AA}^{-1} < q < 0.05 \text{ \AA}^{-1}$

**Table S2. Properties Derived by SANS. Related to Figure 4.**

Sample	Guinier		GNOM		Mass (kD)		Apparent Oligomer
	qR <sub>g</sub>	R <sub>g</sub> ( $\text{\AA}$ )	R <sub>g</sub> ( $\text{\AA}$ )	D <sub>max</sub> ( $\text{\AA}$ )	By Q <sub>r</sub> <sup>3</sup>	By Porod <sup>1</sup>	
5 mg/mL IN <sup>Y15A,F185H</sup>	0.52 – 1.32	39.5 $\pm$ 1.8	36.3 $\pm$ 0.76	111	22.9	30.6	Dimer

<sup>1</sup>Porod Volume ( $V_p$ ). This figure can be used to estimate the mass of compact proteins, where  $V_p/1.6 \sim \text{MM}$ .

<sup>2</sup>Porod exponent. Values near  $\sim 4$  indicate compactness, whereas lower values between  $< 2-3$  indicate significant lack of compactness and increased volumes (Rambo and Tainer, 2011). These values were determined using the program ScÅtter (<https://bl1231.als.lbl.gov/scatter/>).

**Table S3. Properties Derived by SEC-SAXS. Related to Figure 6.**

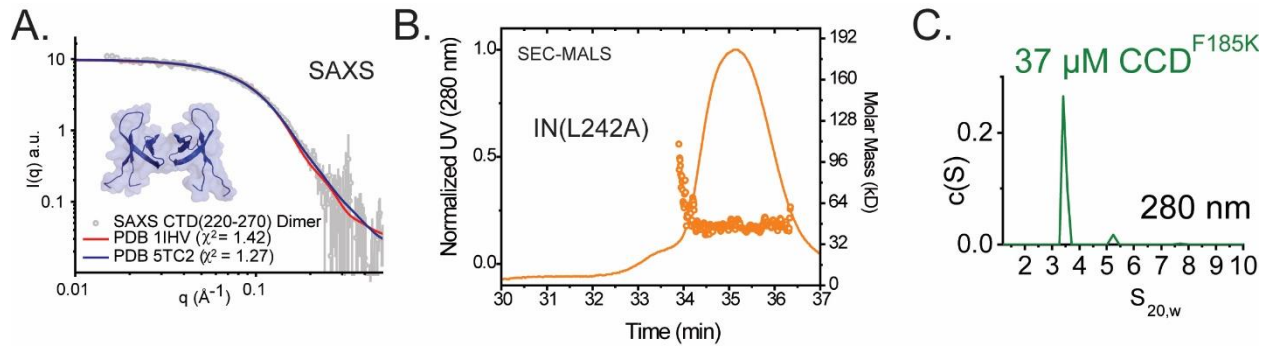
Sample	Guinier		GNOM		P <sub>x</sub> <sup>2</sup>	Mass (kD)		Oligomer
	qR <sub>g</sub>	R <sub>g</sub> ( $\text{\AA}$ )	R <sub>g</sub> ( $\text{\AA}$ )	D <sub>max</sub> ( $\text{\AA}$ )		By Q <sub>r</sub> <sup>3</sup>	By Porod <sup>1</sup>	
IN(CCD) <sup>F185K</sup>	0.32 – 1.31	21.3 $\pm$ 0.06	21.3 $\pm$ 0.08	72	3.7	34.0	37.0	Dimer
	0.47 – 1.27	18.1 $\pm$ 0.36	19.1 $\pm$ 0.16	52	2.4	19.5	18.0	Monomer
IN(CTD)220-270	0.32 – 1.32	17.9 $\pm$ 0.23	18.2 $\pm$ 0.33	63	4.0	15.3	15.1	Dimer
	0.53 – 1.32	17.5 $\pm$ 0.01	17.1 $\pm$ 0.04	50	2.5	9.0	7.0	Monomer
IN(CTD)220- 270 <sup>L242A</sup>	0.51 – 1.35	19.2 $\pm$ 0.23	18.2 $\pm$ 0.33	66	1.5	14.9	15.0	Dimer
	0.57 – 1.33	19.1 $\pm$ 0.87	17.1 $\pm$ 0.04	50	1.7	8.4	6.9	Monomer
IN(CTD)220-288	0.51 – 1.35	21.8 $\pm$ 0.01	18.2 $\pm$ 0.33	82	2.4	17.6	17.9	Dimer
	0.36 – 1.35	15.7 $\pm$ 0.05	17.1 $\pm$ 0.04	64	2.5	8.8	6.7	Monomer

<sup>1</sup>Porod Volume ( $V_p$ ). This figure can be used to estimate the mass of compact proteins, where  $V_p/1.6 \sim \text{MM}$ .

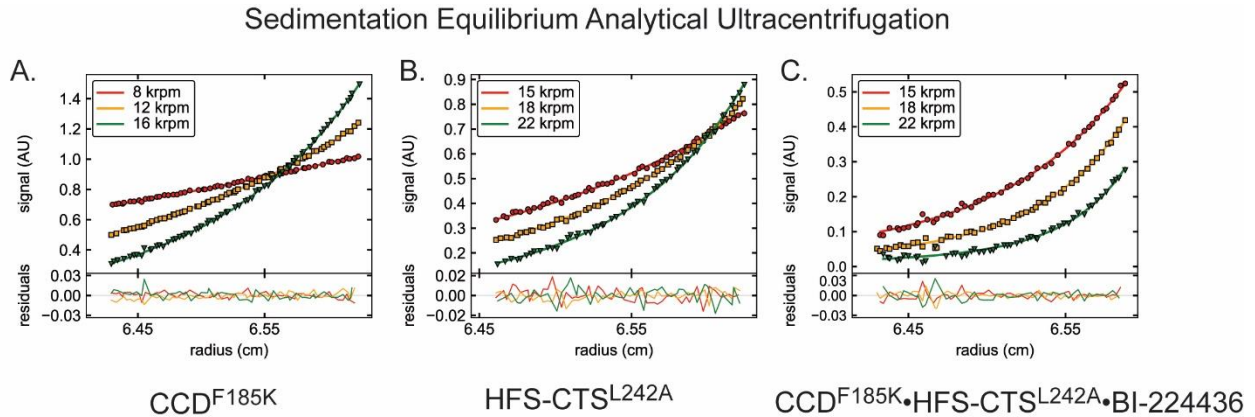
<sup>2</sup>Porod exponent. Values near  $\sim 4$  indicate compactness, whereas lower values between  $< 2-3$  indicate significant lack of compactness and increased volumes (Rambo and Tainer, 2011). These values were determined using the program ScÅtter (<https://bl1231.als.lbl.gov/scatter/>).

<sup>3</sup>Mass determinations (MM) using the Q<sub>r</sub> invariant (Rambo and Tainer, 2013) were determined using the program RAW(Hopkins et al., 2017).

<sup>3</sup>Mass determinations (MM) using the  $Q_r$  invariant (Rambo and Tainer, 2013) were determined using the program RAW(Hopkins et al., 2017).



**Sfig 1. Biophysical properties of IN domains and variants (Related to Figures 6 and 7).** A. Confirmation of the CTD Dimer structure by SEC-SAXS. Shown in grey is the deconvoluted SAXS data for the CTD dimer. Shown in solid lines are the CRYSOLOG fits to the data with the experimental crystallographic (blue) and NMR (red) structures for the CTD Dimer. B. Effects of L242A on full-length  $IN^{F185H}$ , as determined by SEC-MALS analysis. The mass profile and retention time are consistent with the presence of monomers and dimers. C. SV-AUC control data on 37  $\mu$ M CCD dimer alone (green), as observed at 280 nm, where a  $\sim 3.5S$  species corresponding to dimer is observed.



**Sfig 2. Sedimentation Equilibrium Analysis (Related to Figure 7).** (A-C) Representative sedimentation equilibrium analytical ultracentrifugation data for (A) 20  $\mu$ M  $CCD^{F185K}$  fit to a single-species model (B) 27  $\mu$ M  $HFS-CTD^{L242A}$  fit to a monomer-dimer model and (C) 20  $\mu$ M  $CCD^{F185K} \cdot HFS-CTD^{L242A} \cdot BI-224436$  fit to an A-B-A association model. Shown in the upper panels are radial absorbance data plotted with fitted models shown as solid lines for each of three speeds. Shown in the respective lower panels are the residuals for each fit. Parameters derived from this analysis are provided in Table S4. Figures were prepared using the program GUSSE.

**Table S4. Properties determined by Sedimentation Equilibrium Analysis (4°C). Related to Figure 7.**

Sample	Speeds (krpm)	Concentration ( $\mu\text{M}$ )	Association Model	Mass (Daltons)	$K_d$	Global Reduced $\chi^2$
CCD <sup>F185K</sup>	8, 12, 16	10, 20, 30	Single Species	36,991 $\pm$ 400	<i>n.a.</i>	1.28
HFS-CTD <sup>L242A</sup>	15, 18, 22	16, 27, 43	M-D		65 $\mu\text{M} \pm 6$	1.17
CCD <sup>F185K</sup> - HFS-CTD <sup>L242A</sup>	15, 18, 22	13, 20, 23	Single Species	33,998	<i>n.a.</i>	1.26
CCD <sup>F185K</sup> • HFS-CTD <sup>L242A</sup> • BI-224436	15, 18, 22	13, 20	Single Species	62,938	<i>n.a.</i>	1.87
CCD <sup>F185K</sup> - HFS-CTD <sup>L242A</sup>	15, 18, 22	13, 20, 23	ABA		$\gg 1$ mM	1.72
CCD <sup>F185K</sup> • HFS-CTD <sup>L242A</sup> • BI-224436	15, 18, 22	13, 20	ABA		0.31 $\mu\text{M} \pm 0.21$	0.90